Supporting Information

Redox Activity and Nano-Bio Interactions Determine the Skin Injury Potential of Co_3O_4-Based Metal Oxide Nanoparticles toward Zebrafish

Guotao Peng[1,2], Yuan He[1,2], Xiaoxiao Wang[1,2], Yan Cheng[3], Haiyuan Zhang[3], Kai Savolainen[4], Lutz Mädler[5,6], Suman Pokhrel[5,6*], Sijie Lin[1,2*]

[1]College of Environmental Science and Engineering, Biomedical Multidisciplinary Innovation Research Institute, Shanghai East Hospital, Tongji University, Shanghai 200092, China
[2]Key Laboratory of Yangtze River Water Environment, Ministry of Education; Shanghai Institute of Pollution Control and Ecological Security, Shanghai 200092, China
[3]Laboratory of Chemical Biology, Changchun Institute of Applied Chemistry, Chinese Academy of Sciences, Changchun, Jilin 130022, China
[4]Finnish Institute of Occupational Health, Helsinki 00250, Finland
[5]Faculty of Production Engineering, University of Bremen, 28359 Bremen, Germany
[6]Leibniz Institute for Materials Engineering IWT, 28359 Bremen, Germany

Address Correspondence to:
Sijie Lin, Ph.D. Professor
College of Environmental Science and Engineering, Tongji University
1239 Siping Road, Shanghai 200092, China
Tel: 86 21 65982325
E-mail: lin.sijie@tongji.edu.cn

Suman Pokhrel, Dr. habil
Faculty of Production Engineering, University of Bremen, Badgasteiner Str. 1, 28359 Bremen, Germany and Leibniz Institute for Materials Engineering IWT, Badgasteiner Str. 3, 28359 Bremen, Germany;
Tel: +49 42121851218
E-mail: spokhrel@iwt.uni-bremen.de

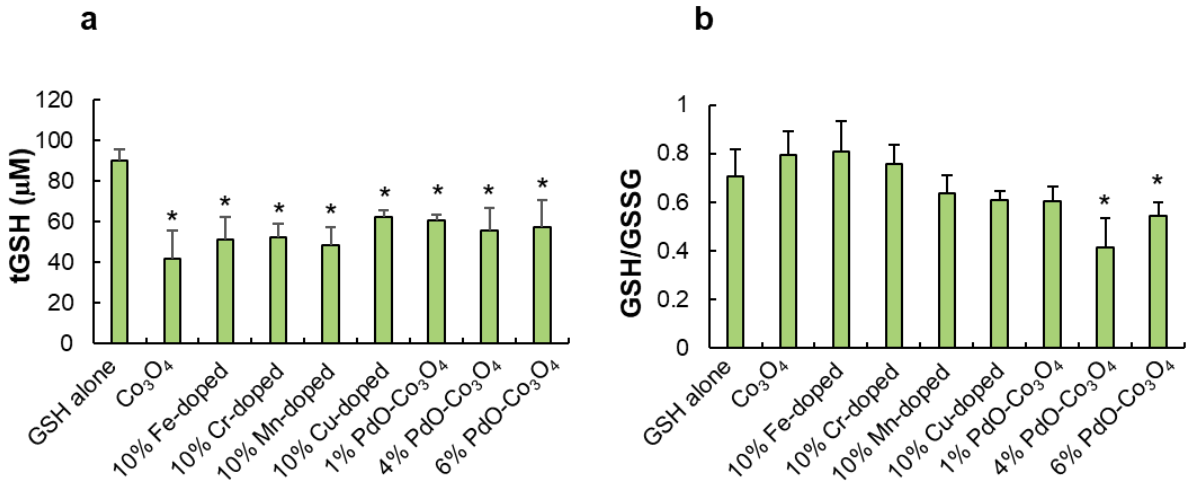

Fig. S1 Total GSH depletion exerted by Co_3O_4-based nanoparticles. a Significant depletion of total GSH was found in all Co_3O_4-based nanoparticles treatment groups due to the abiotic ROS generation. There were no statistically significant differences among treatment groups. **b** Significantly lowered GSH/GSSG ratios were found after treatment in 4% and 6% PdO-Co_3O_4 nanoparticles. Amount of 100 μM GSH was mixed with each type of Co_3O_4 nanoparticles at 100 ppm for 6 h. The GSH was determined by a commercial GSH assay kit (Nanjing Jiancheng Bioengineering Institute, Nanjing, Jiangsu Province, China). A stock of 200 μM GSH was freshly prepared prior to each use. The final concentration of GSH and Co_3O_4-based nanoparticles used were 100 μM and 100 ppm, respectively. GSH alone was used as a negative control. After incubation for 6 h at 28 ℃, the supernatant was collected by centrifuging at 9600 *g* for 5 min for quantification of total GSH and GSSG, based on a chromogenic reaction with 5,5'-dithiobis-2-nitrobenzoic acid (DTNB). The absorbance at 405 nm was read on the microplate reader, and the concentration of total GSH, GSSG and reduced GSH were calculated according to the manufacturer's instructions. Student's T-test was used to evaluate the statistically significant differences of total GSH, GSH/GSSG ratios between the treatments and the negative control group. Statistically significant differences were considered when $p < 0.05$.

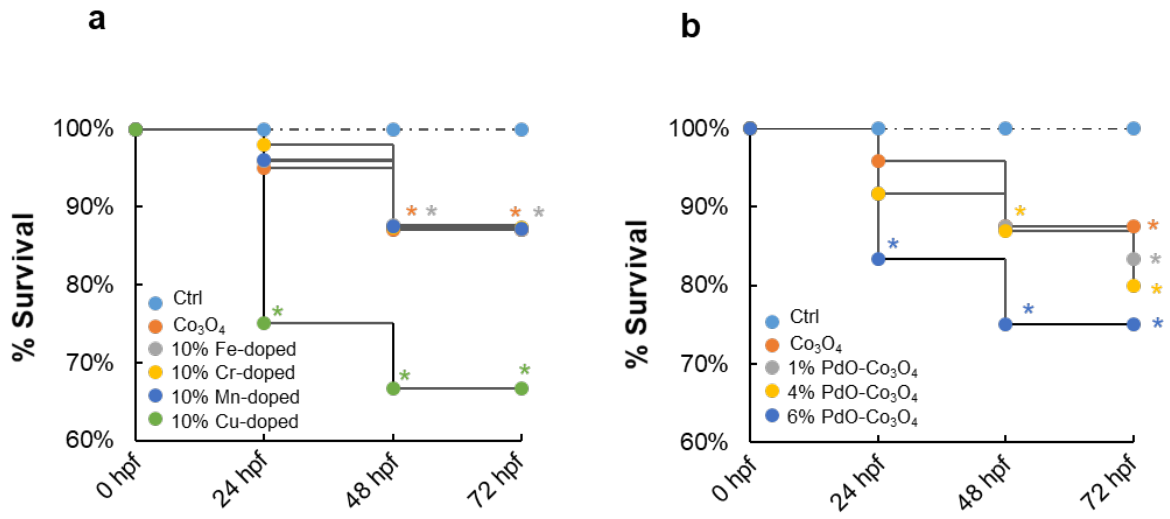

Fig. S2 Mortality of dechorionated embryos exerted by Co_3O_4-based nanoparticles. a Survival rate of dechorionated embryos decreased with the increase of exposure time. At 20 h post exposure (24 hpf), significant lowered survival rate was found in embryos exposed to Cu-doped Co_3O_4 at 100 ppm. With increasing exposure time, the survival rate continued to drop to ~65% after another 24 h (48 hpf). Embryos exposed to Mn-doped, Cr-doped, and Fe-doped Co_3O_4 maintained the survival rate of approximately 90%. **b** In the case of PdO-Co_3O_4 exposed embryos, it also showed a decreasing survival rate with increasing exposure time. Also, the survival rate decreased with the amount of PdO, with 6% PdO-Co_3O_4 being the most detrimental one, followed by 4% and 1% PdO-Co_3O_4 nanoparticles.

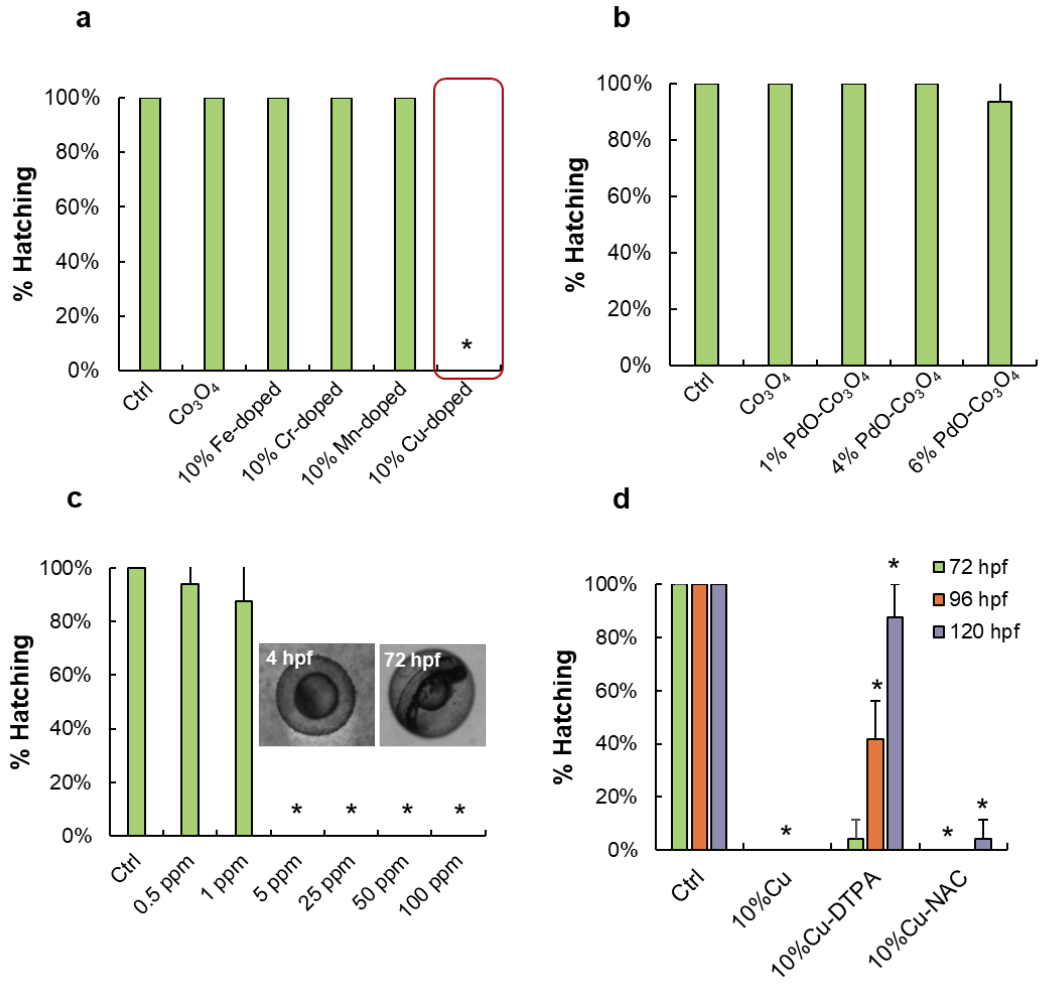

Fig. S3 Hatching interference of Co_3O_4-based nanoparticles in zebrafish embryos. a In transition metal doped library, significant hatching interference was only observed in Cu-doped Co_3O_4 exposed embryos at 100 ppm. **b** In the case of PdO-Co_3O_4 exposed embryos, no observable hatching interference was found. **c** Concentration-dependent hatching interference exerted by Cu-doped Co_3O_4 nanoparticles. Cu-doped Co_3O_4 exerted hatching interference at and above 5 ppm. **d** When embryos were co-exposed to 100 ppm of Cu-doped Co_3O_4 with metal ion chelator, DTPA at 100 μM was sufficient to reverse the hatching interference effects. While co-exposure with ROS scavenger NAC did not have any protective effect against hatching interference, indicating that the hatching interference was mostly due to the metal ion shedding rather than the ROS generation.

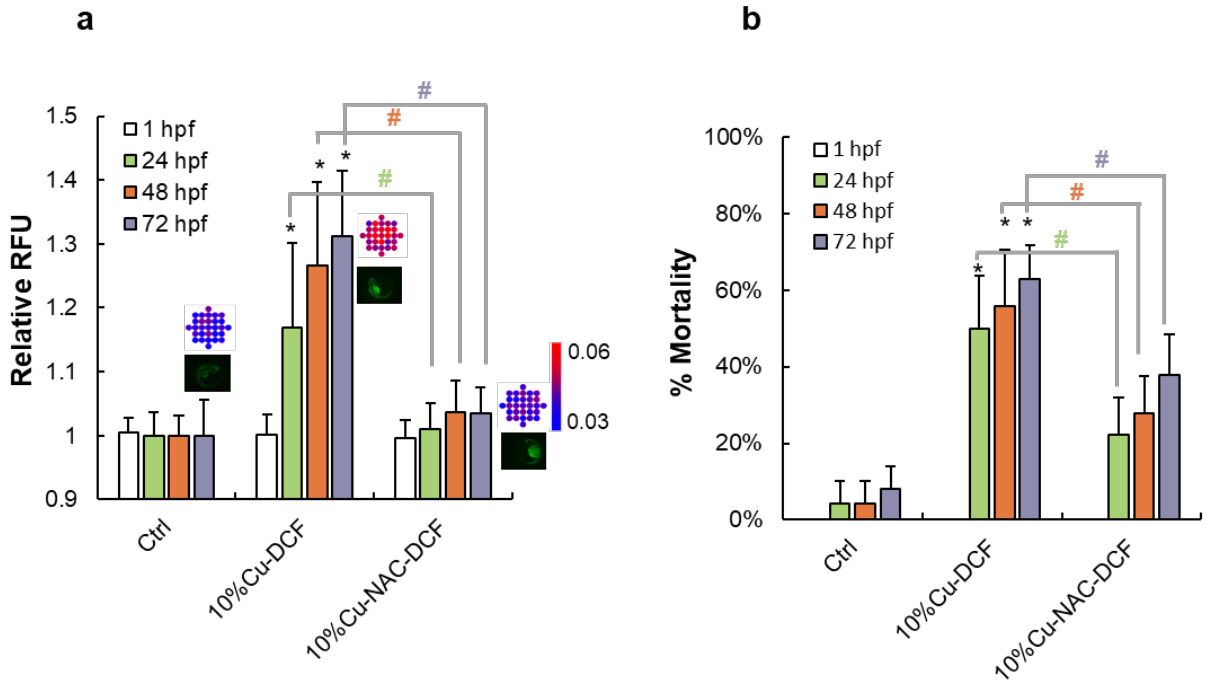

Fig. S4 Toxicity assessment of Co_3O_4-based nanoparticles in zebrafish embryos through microinjection. a Use of DCF to assess the biotic ROS on embryos after microinjection to chorionic sac with Cu-doped Co_3O_4 nanoparticles at 100 ppm. Significant increase of biotic ROS was found after nanoparticles was injected, indicated by DCF fluorescence, and the ROS scavenger NAC was able to sequester the extensive ROS effectively. **b** Microinjection of Cu-doped Co_3O_4 nanoparticle to chorionic sac resulted in significant mortality compared to control, and co-injection of NAC mitigated the mortality *via* attenuation of ROS generation, with the concentration of 100 μM. A mixture of H_2DCFDA and Cu-doped Co_3O_4 nanoparticles were co-injected into embryos chorionic sac at 1 hpf, with the concentration of 10 μM and 100 ppm, respectively. NAC with the concentration of 100 μM were co-injected as ROS scavenger. The biotic ROS generation was determined by the DCF fluorescence intensity using a microplate reader. The average fluorescence value of 29 multiple points was presented and all the data was normalized to control before statistical analysis. The mortality rate was assessed at each testing point accordingly.

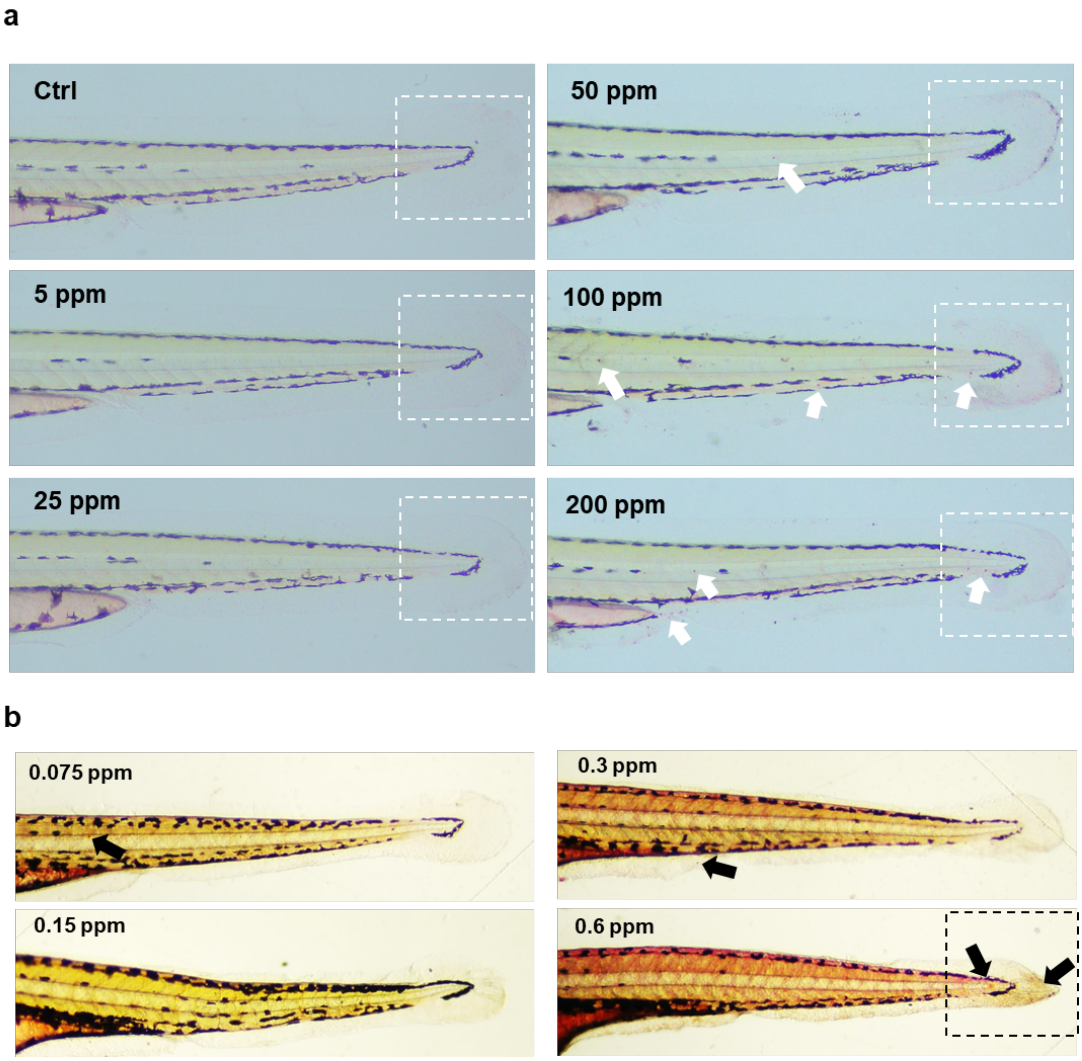

Fig. S5 Larval Skin injury exerted by Cu-doped Co_3O_4 nanoparticles and $CuCl_2$. a Zebrafish developing larvae at 72 hpf were exposed to Cu-doped Co_3O_4 nanoparticles at 5, 25, 50, 100 and 200 ppm for 2 hours, respectively. After the exposure, the larvae were collected, washed and incubated with 25 μgmL^{-1} neutral red for 20 min. Bright-field images were captured after gently washing the larvae three times in Holtfreter's medium. The injured cells on the zebrafish larval skin were stained in red. Skin and tail fin injury were observed at 50 ppm and above, indicated by the arrows. **b** Skin injury exerted by $CuCl_2$ salt in zebrafish larvae.

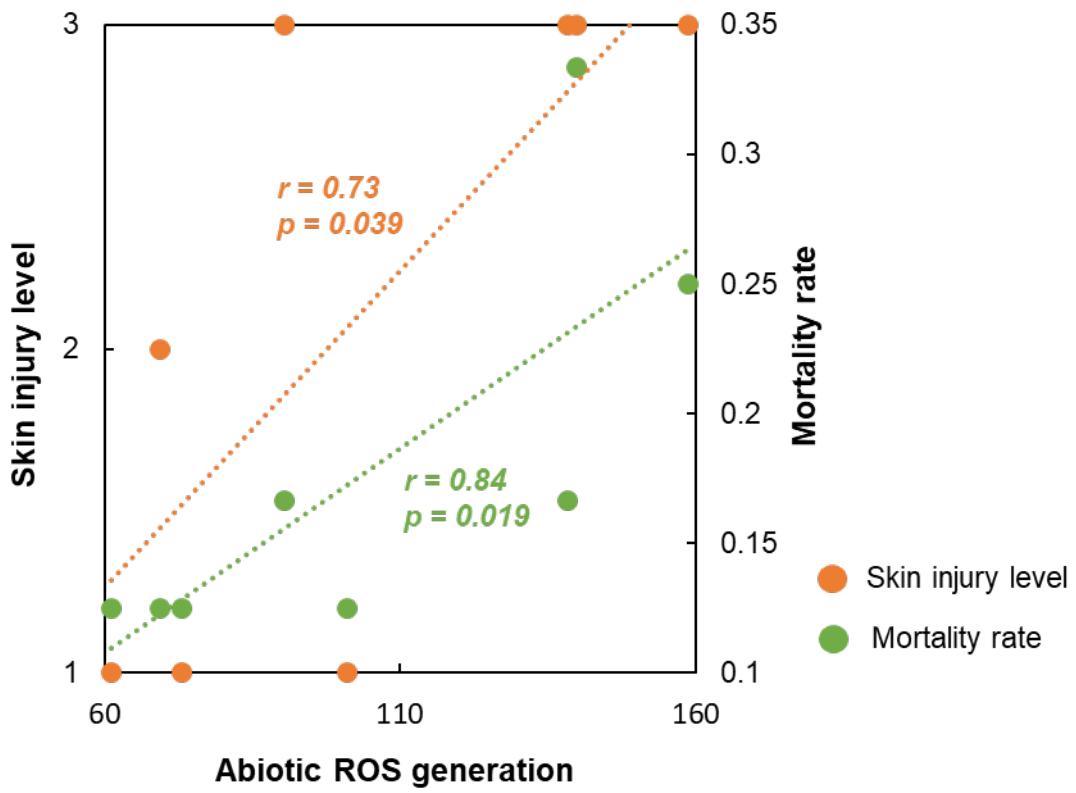

Fig. S6 Pearson correlation analyses of abiotic total ROS generated by two libraries of Co_3O_4-based nanoparticles *vs.* mortality embryos or skin injury levels of hatched larvae. The skin injury levels were numerical as "1, 2, 3" in accordance with the injury level "+, ++, +++" presenting in Fig. 2b. A significant positive correlation was found between the mortality of dechorionated embryos and the abiotic ROS generation, with Pearson *r* being 0.73 (*p = 0.039*). Same trend was observed between the larvae skin injury level and the abiotic ROS, with Pearson *r* being 0.84 (*p = 0.019*).

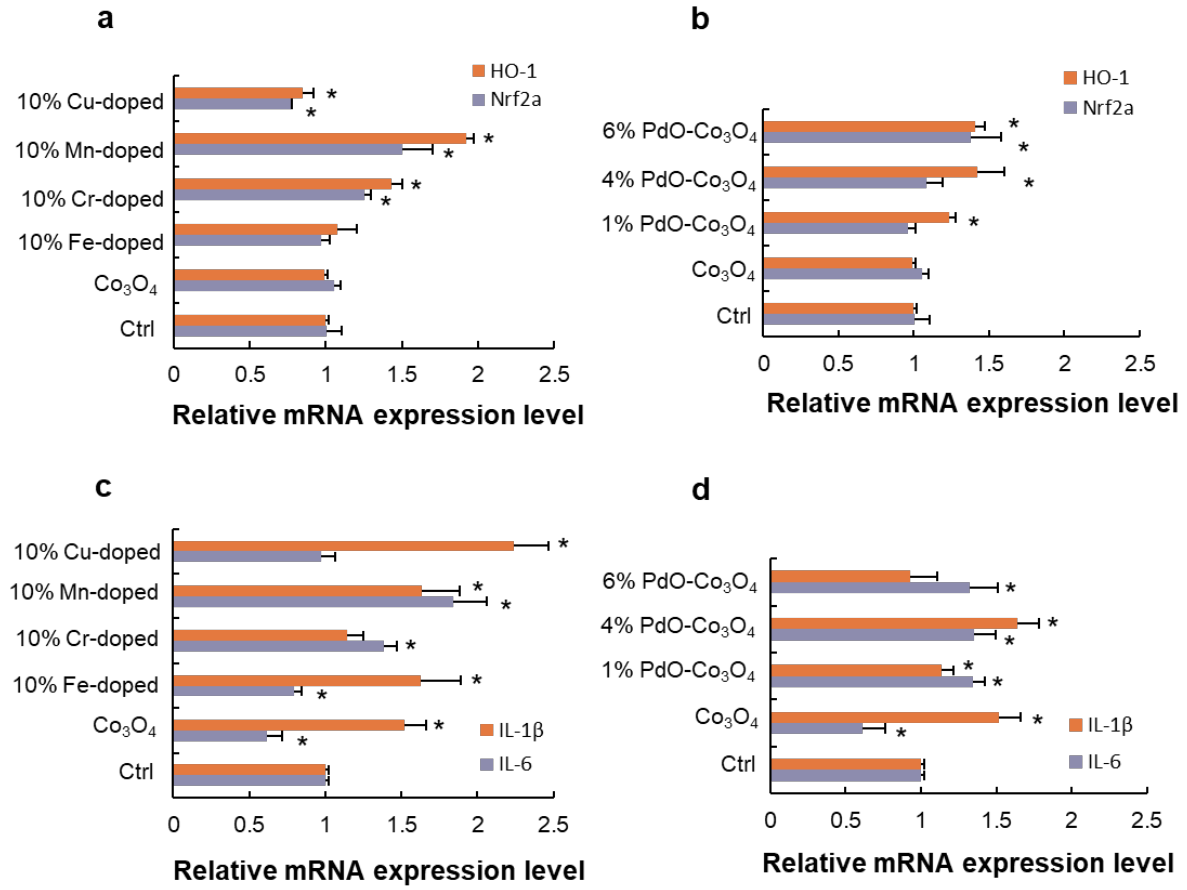

Fig. S7 Relative mRNA expression levels of genes related to oxidative stress in zebrafish. *β-action* was used as the housekeeping gene. **a** In the transition metal doped-Co_3O_4 exposed larvae, significant increases of *Nrf2a* and *HO-1* mRNA expression were observed for Cr- and Mn-doped Co_3O_4 nanoparticles compared to the control. **b** In the case of PdO-Co_3O_4 nanoparticles, the trend of *Nrf2a* and *HO-1* mRNA expression was in consistent with the amount of PdO, indicating the presence of heterojunction facilitated the oxidative stress in zebrafish. **c** Relative mRNA expression levels of *IL-1β* and *IL-6* in transition metal-doped Co_3O_4 exposed larvae. Significant increase of *IL-1β* was observed in larvae exposed to pure and transition metal doped-Co_3O_4 nanoparticles, and the most pronounced relative expression level was observed in 10% Cu-doped Co_3O_4 treated group. **d** The transcription of *IL-6* and *IL-*

1β genes was significantly raised in all PdO-Co_3O_4 treatments (except the *IL-1β* transcription in 6% PdO treatment), suggesting the heterojunctions exacerbating the oxidative stress to pro-inflammation.

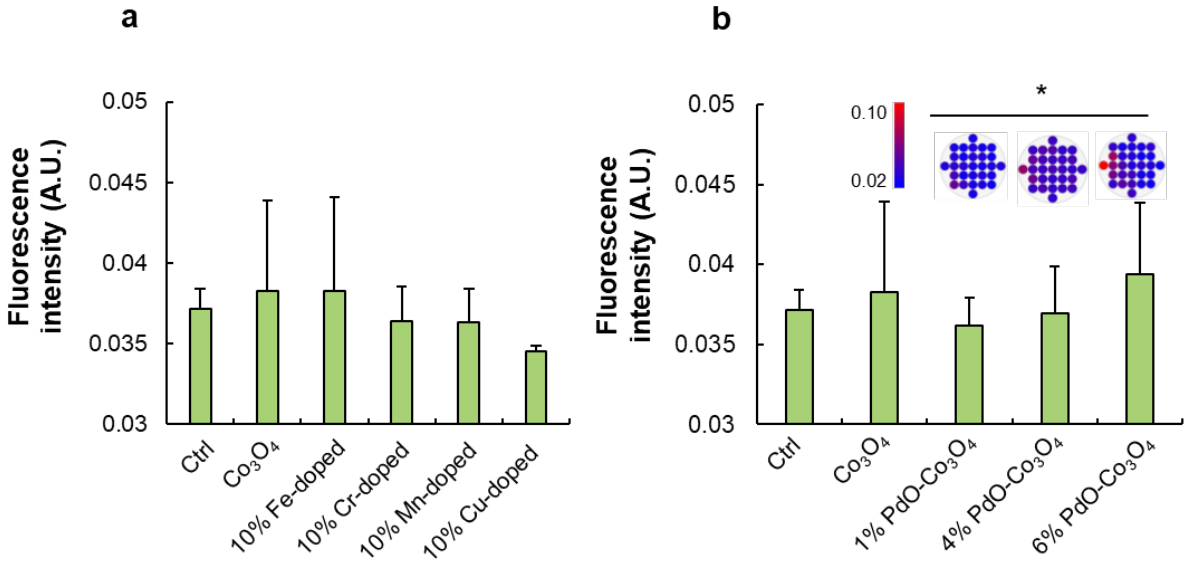

Fig. S8 Biotic ROS assessment of 72 hpf zebrafish developing larvae after exposure to Co_3O_4-based nanoparticles. a In transition metal doped-Co_3O_4 nanoparticles exposed larvae, no significant differences were found compared to the control. **b** In the case of PdO-Co_3O_4 exposed larvae, the biotic ROS generation increased with the amount of PdO, labeled by the DCF fluorescence intensity. The detached chorions of zebrafish embryo at 4 hpf were exposed to Co_3O_4-based nanoparticles at 100 ppm. The surviving developing larvae at 72 hpf were collected and transfer to 96-well plate for biotic ROS assessment through optic bottom reading on a microplate reader. The average of 29 multiple points was used for each well fluorescence value, demonstrated as the heatmaps in the figure.

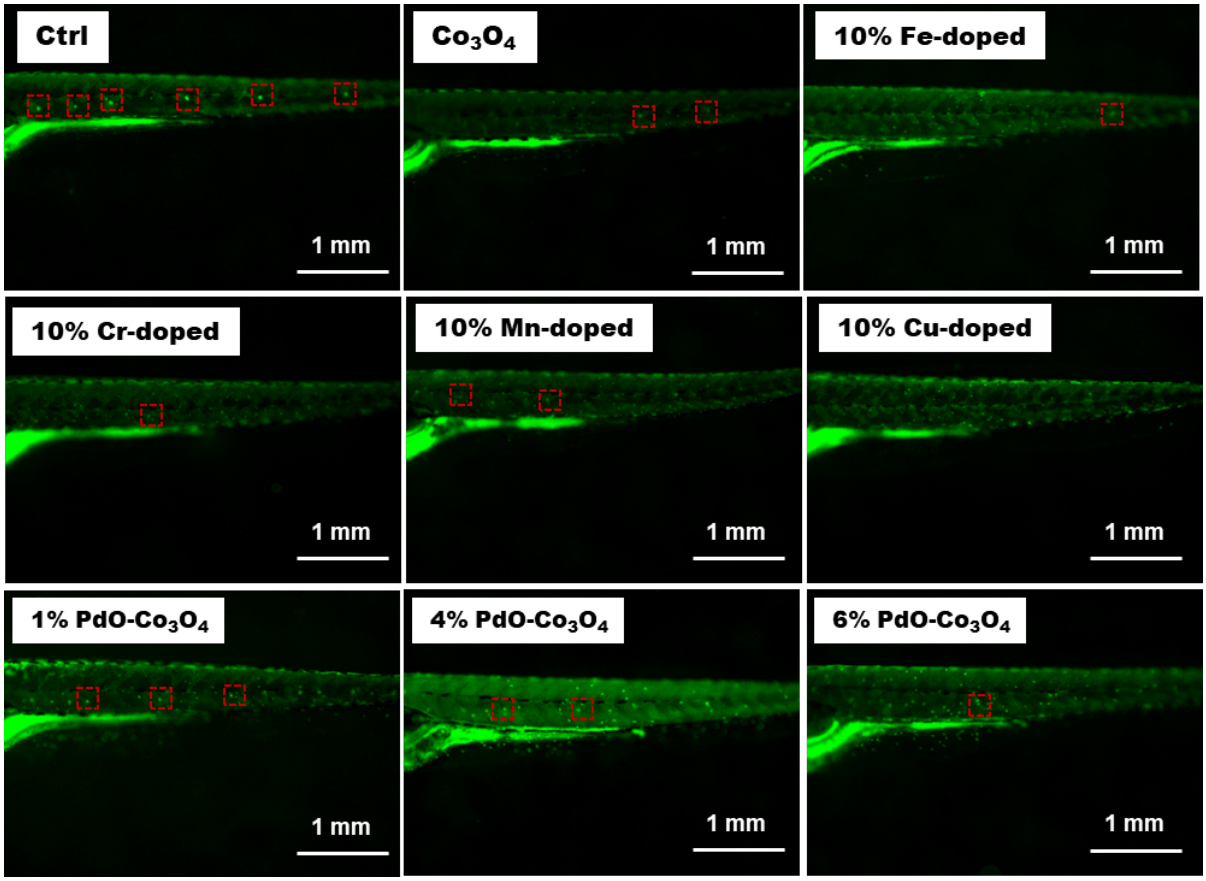

Fig. S9 Use of DASPEI to determine the hair cells injury in 6 dpf zebrafish larvae. Each Co_3O_4-based nanoparticle was found to cause recognizable injury to the neuromasts hair cells in zebrafish, with Cu-doped Co_3O_4 being the most detrimental one. Zebrafish larvae at 6 dpf were exposed to Co_3O_4-based nanoparticles at 200 ppm for 2 h. After the exposure, larvae were rinsed three times in Holtfreter's medium, and incubated with 50 μgmL^{-1} of DASPEI for 15 min. Labeled larvae were then rinsed, anaesthetized using 0.01% tricaine and positioned in 1% low-melt agarose gel for fluorescent imaging with FITC filter set (Ex: 488 nm, Em: 540 nm).

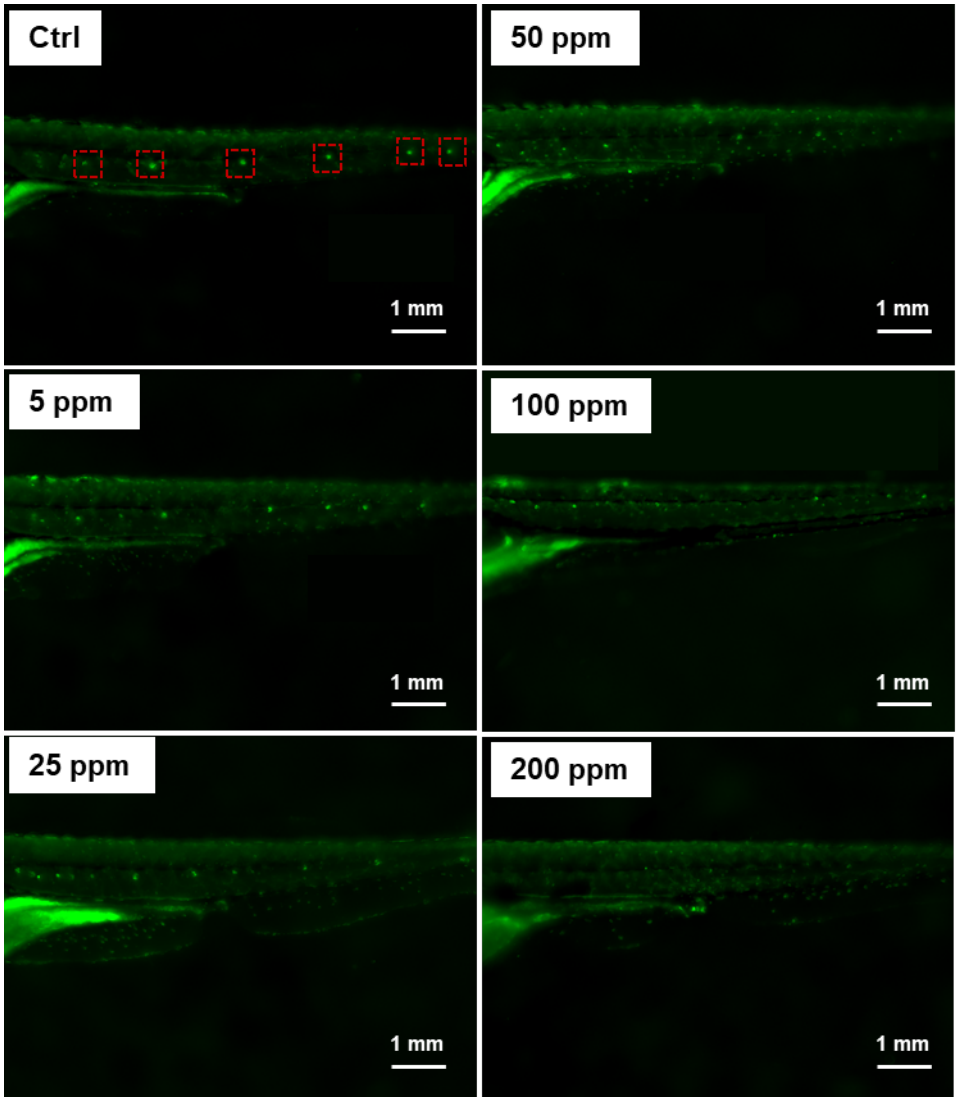

Fig. S10 Use of DASPEI to determine the hair cells injury in 6 dpf zebrafish larvae exerted by Cu-doped Co_3O_4 nanoparticles. Significant neuromasts hair cells injury was observed at 100 ppm and above. Zebrafish larvae were exposed in Cu-doped Co_3O_4 nanoparticles at different concentrations of 5, 25, 50, 100 and 200 ppm for 2 hours. After the exposure, larvae were rinsed three times in Holtfreter's medium, and incubated with 50 μgmL^{-1} of DASPEI for 15 min. Labeled larvae were then rinsed, anaesthetized using 0.01% tricaine and positioned in 1% low-melt agarose gel for fluorescent imaging with FITC filter set (Ex: 488 nm, Em: 540 nm).

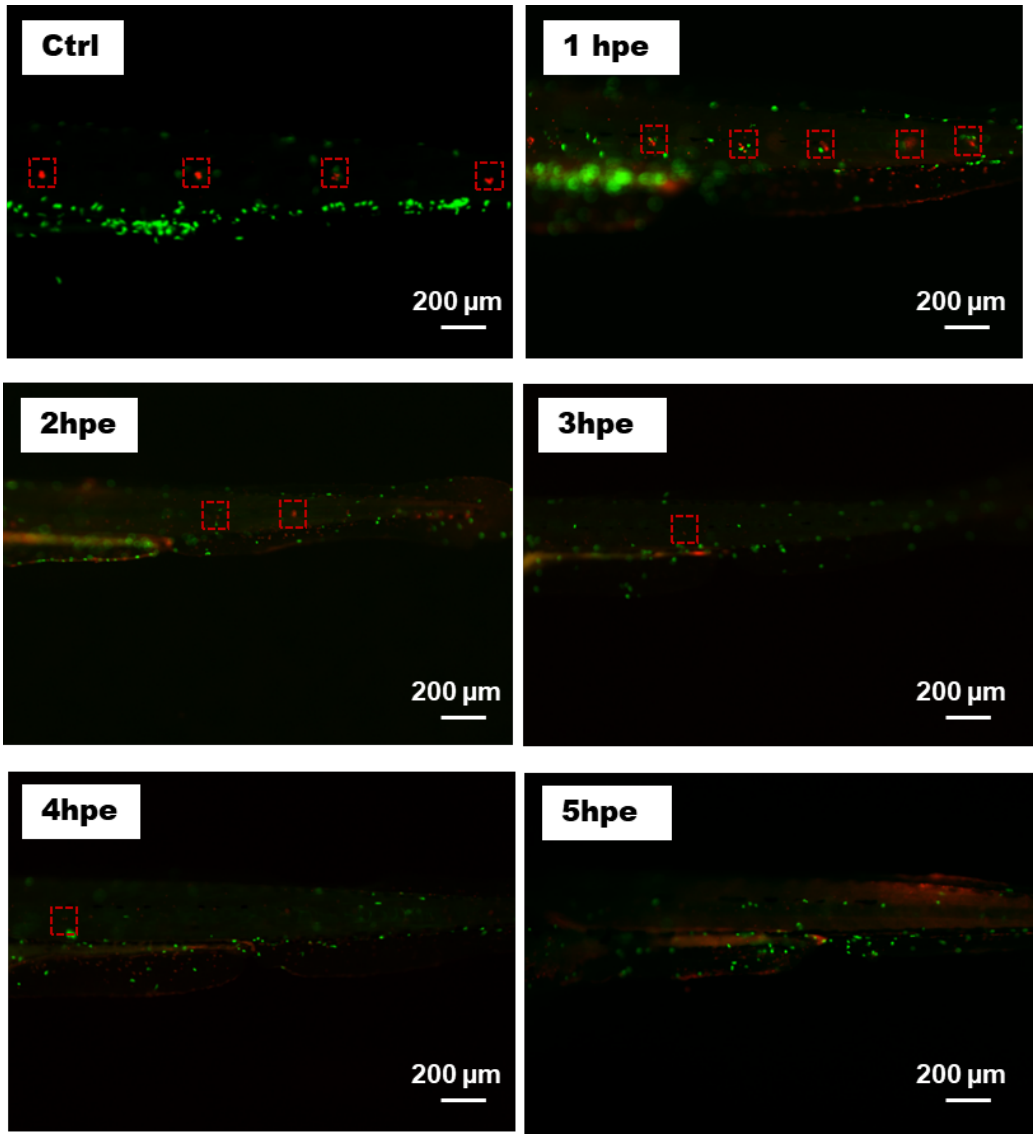

Fig. S11 Use of DASPEI to determine the hair cells injury in 6 dpf zebrafish larvae exerted by 6% PdO-Co_3O_4 nanoparticles. The injury level was time dependent; larvae exposed to 200 ppm 6% PdO-Co_3O_4 nanoparticles for 5 h showed a complete loss of neuromasts hair cells. Zebrafish larvae at 6 dpf were exposed to 6% PdO-Co_3O_4 nanoparticles at 200 ppm for 1, 2, 3, 4 and 5 h, respectively. After the exposure, larvae were rinsed three times in Holtfreter's medium, and incubated with 50 µgmL^{-1} of DASPEI for 15 min. Labeled larvae were then rinsed, anaesthetized using 0.01% tricaine and positioned in 1% low-melt agarose gel for fluorescent imaging with FITC filter set (Ex: 488 nm, Em: 540 nm).

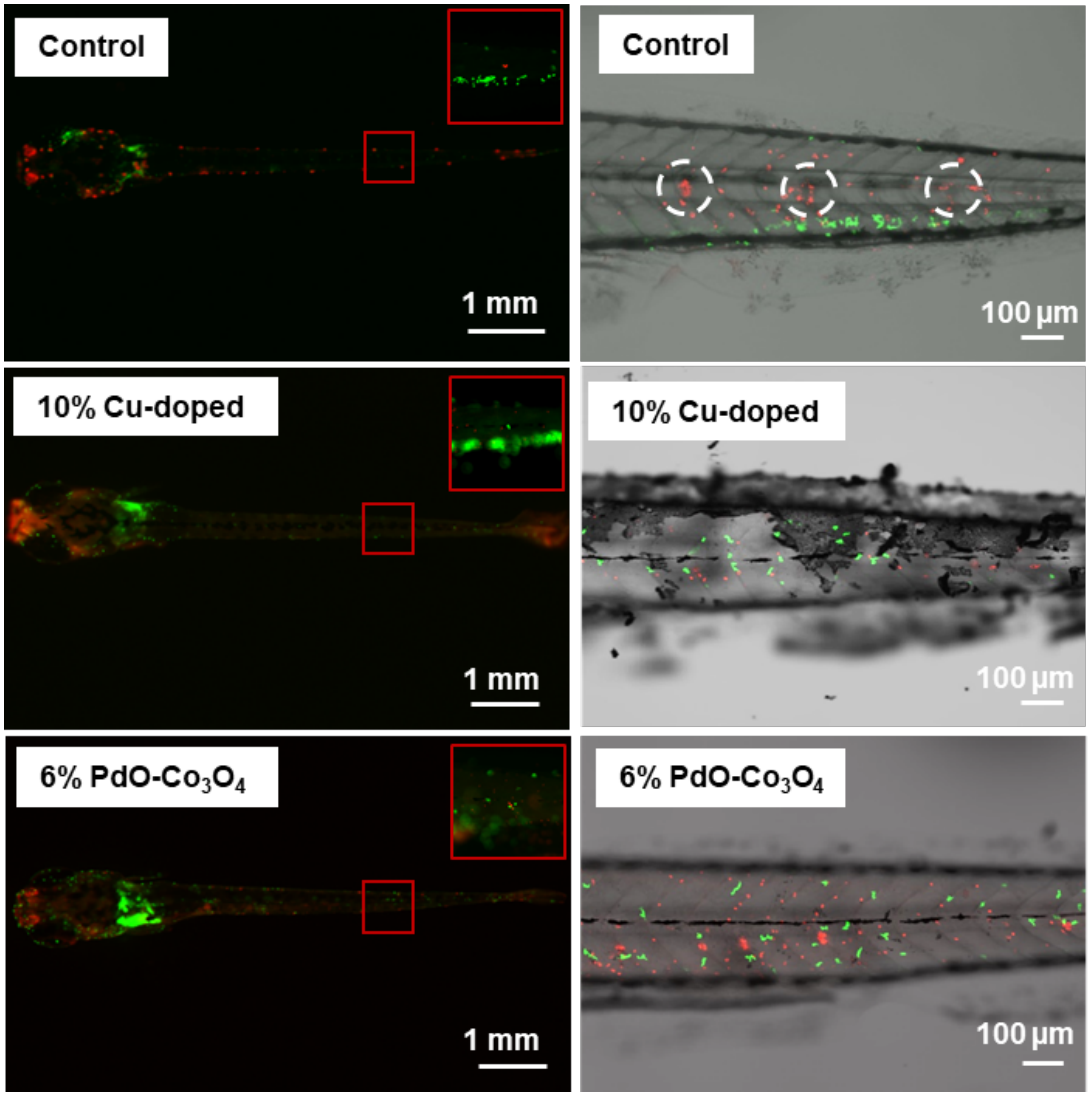

Fig. S12 Inflammatory responses of zebrafish larvae after exposure to Co_3O_4-based nanoparticles. Use of DASPMI (4-Di-1-ASP) to stain the hair cells on 6 dpf *Tg*(*LysC:eGFP*) zebrafish larvae. Hair cells were identified with the red fluorescent dye, DASPMI, and the movement of immune cells was visualized with GFP-positive macrophages and neutrophils. Hair cells cluster were lost and the migration of immune cells to the larval neuromasts was observed after 1 h exposure of 10% Cu-doped Co_3O_4 and 6% PdO- Co_3O_4 nanoparticles at 200 ppm, respectively. Images were captured by both epifluorescence and Confocal fluorescence microscopes.

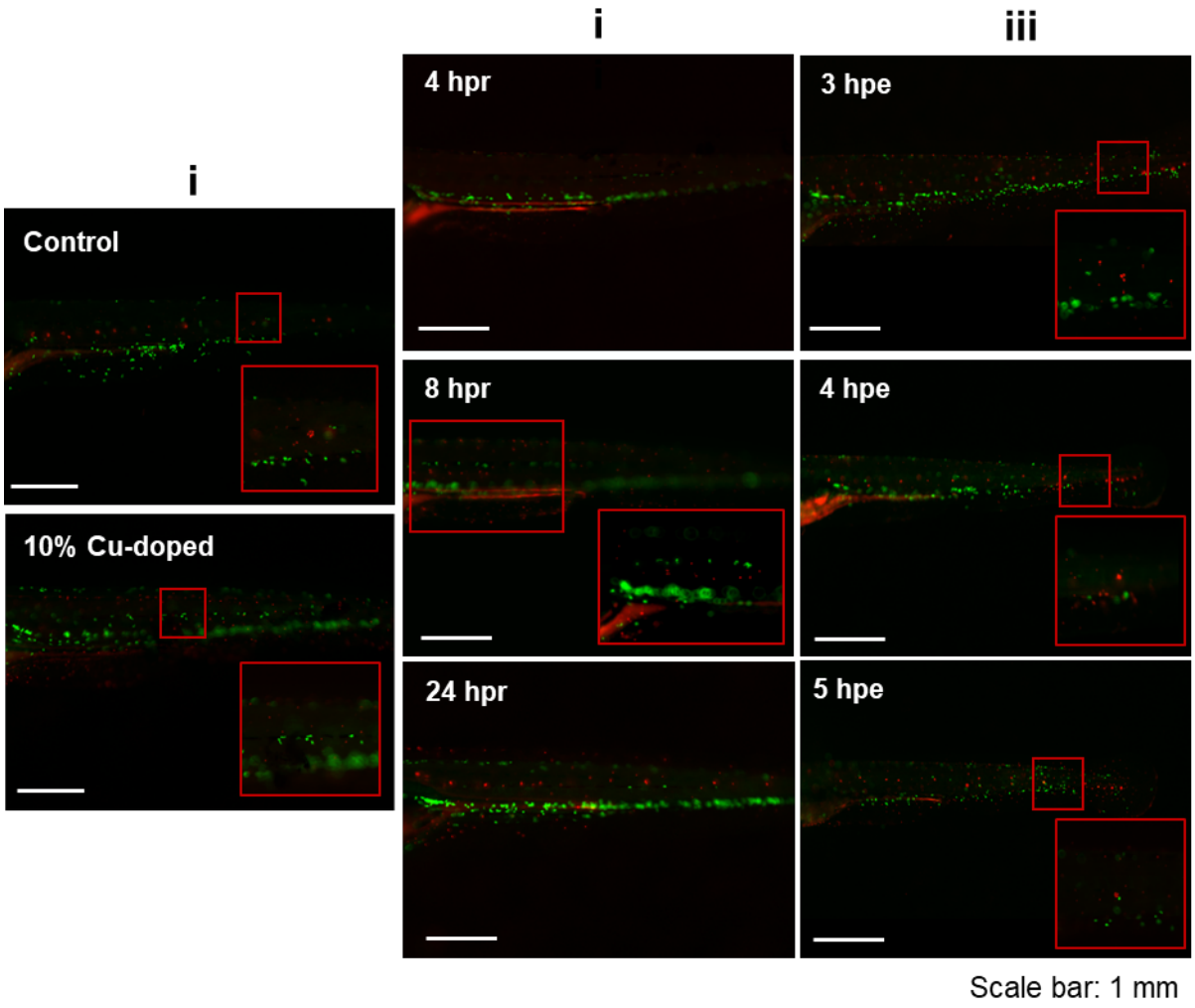

Fig. S13 Skin injury in zebrafish larvae was recoverable after recuperating in fresh Holtfreter's medium. (i) Exposure in Cu-doped Co_3O_4 at 200 ppm for 2 h resulted in a complete wipe out of neuromasts hair cells. (ii) Recovery timeline of hair cells in fresh Holtfreter's medium after exposure to Cu-doped Co_3O_4 for 2 h. Parts of the hair cells clusters were able to regenerate 8 h post-recovery (hpr) and all of the hair cells recovered 24 h post-recovery. (iii) Zebrafish neuromasts hair cells could recover after 24 h recuperating in fresh Holtfreter's medium even after 5 h post-exposure (hpe) in Cu-doped Co_3O_4 nanoparticles at 200 ppm.

Video S1 A time-lapse video to trace the immune cells in transgenic zebrafish *Tg*(*LysC:*eGFP). GFP-positive macrophages and neutrophils were mostly located in the vasculature, with majority of them attached to the endothelial wall of blood vessels. A small number of GFP-positive cells were observed to occasionally de-attach from the endothelial wall and perform immune surveillance throughout the body. Fluorescence images were captured with FITC filter set (Ex: 488 nm, Em: 540 nm) under a fluorescence microscope (Olympus-SZ2-ILA, Olympus Ltd., Japan). Time-lapse action was performed with the settings of one image per min and the total time as 2 h, thus 120 pictures in total to capture the immune cells movement.

Video S2 A time-lapse video to clarify the interactions between the immune cells and hair cells in transgenic zebrafish *Tg*(*LysC:*eGFP). During the observed time frame, the immune cells showed clear active movement around the injured neuromasts hair cells at the larval skin. 6 dpf transgenic zebrafish *Tg*(*LysC:*eGFP) were exposed to Cu-doped Co_3O_4 nanoparticles at 200 ppm for 2 h. After the exposure, larvae were rinsed three times with Holtfreter's medium and incubated with 50 μgmL^{-1} of DASPMI for 15 min. Labeled larvae were then rinsed, anaesthetized using 0.01% tricaine and positioned in 1% low-melt agarose gel for fluorescent imaging under a Confocal Laser Scanning Microscope (FV3000, Olympus Ltd., Japan). Time-lapse action was performed with the settings of one image per min and the total time as 2 h, thus 120 pictures in total to observe the interactions between the immune cells and hair cells.

Video S3 A time-lapse video to trace the immune cells migration in transgenic zebrafish *Tg*(*LysC:*eGFP) after injured by the nanoparticles. It clearly showed an active recruitment of immune cells along the lateral line 2 h post-recovery. Zebrafish larvae were exposed to Cu-doped Co_3O_4 at 200 ppm for 2 h. After the exposure, larvae were rinsed and transferred to fresh Holtfreter's medium for recovery. After two hours, the injured larvae were anaesthetized, positioned, and observed under a fluorescence microscope (Olympus-SZ2-ILA, Olympus Ltd., Japan). Time-lapse action was performed with the settings of one image per min and the total time as 2 h, thus 120 pictures in total to capture the immune cells migration.

Table S1 Primers of the target genes in this study.

Target genes	Primers	Size (bp)
Nrf2a-F	GAGCGGGAGAAATCACACAGAATG	83
Nrf2a-R	CAGGAGCTGCATGCACTCATCG	
HO-1-F	GGAAGAGCTGGACAGAAACG	107
HO-1-R	CGAAGAAGTGCTCCAAGTCC	
IL-6-F	TCAACTTCTCCAGCGTGATG	73
IL-6-R	TCTTTCCCTCTTTTCCTCCTG	
IL-1β-F	TGGACTTCGCAGCACAAAATG	150
IL-1β-R	GTTCACTTCACGCTCTTGGATG	
β-actin-F	GGATGCGGAAACTGGCAAAG	114
β-actin-R	GAGGGCAAAGTGGTAAACGC	

Table S2 Pearson correlation analyses between the abiotic ROS and biological injuries in zebrafish. Statistical significant differences were considered when *p* values were lower than 0.05.

Pearson correlation analysis			**Pearson correlation coefficient**	***p value***
Abiotic ROS *vs.* Biological injuries in zebrafish	Abiotic ROS *vs.* Survival rate of embryos		**-0.84**	**0.019**
	Abiotic ROS *vs.* Skin injury level in larvae		**0.73**	**0.039**
Microinjection	Biotic ROS *vs.* Mortality		**0.91**	**5.97E-4**
Biotic ROS *vs.* mRNA transcription	Transition metal-doped Co_3O_4	***Nrf 2a***	**0.78**	**0.116**
		HO-1	-0.37	0.537
		IL-1β	-0.23	0.712
		IL-6	-0.55	0.332
	PdO-Co_3O_4	***Nrf 2a***	**0.99**	**0.045**
		HO-1	**0.95**	**0.208**
		IL-1β	-0.22	0.862
		IL-6	-0.88	0.311

Table S3 Pearson *r* value of multiple variable analyses between the physicochemical characteristics of Co_3O_4-based nanoparticles and biological injuries in zebrafish.

Pearson r	Mortality rate	Skin injury level	Abiotic ROS	Surface area	Particle size	Crystallite size	DLS	Zeta potential
Mortality rate	1.00	0.69	0.84	-0.61	0.50	0.07	0.56	-0.72
Skin injury level	0.69	1.00	0.73	-0.82	0.66	-0.42	0.68	-0.67
Abiotic ROS	**0.84**	**0.73**	1.00	-0.66	0.33	0.04	0.51	-0.75
Surface area	-0.61	-0.82	-0.66	1.00	-0.90	0.66	-0.51	0.76
Particle size	0.50	0.66	0.33	-0.90	1.00	-0.75	0.45	-0.65
Crystallite size	0.07	-0.42	0.04	0.66	-0.75	1.00	-0.33	0.26
DLS	0.56	0.68	0.51	-0.51	0.45	-0.33	1.00	-0.73
Zeta potential	-0.72	-0.67	-0.75	0.76	-0.65	0.26	-0.73	1.00

Table S4 *p* values of multiple variable analyses between the physicochemical characteristics of Co_3O_4-based nanoparticles and biological injuries in zebrafish.

P value	Mortality rate	Skin injury level	Abiotic ROS	Surface area	Particle size	Crystallite size	DLS	Zeta potential
Mortality rate	0.00	0.06	0.03	0.11	0.20	0.88	0.14	0.14
Skin injury level	0.06	0.00	0.04	0.01	0.07	0.30	0.06	0.07
Abiotic ROS	**0.02**	**0.04**	0.00	0.08	0.43	0.92	0.20	0.03
Surface area	0.11	0.01	0.08	0.00	0.00	0.07	0.19	0.03
Particle size	0.20	0.07	0.43	0.00	0.00	0.03	0.27	0.08
Crystallite size	0.88	0.30	0.92	0.07	0.03	0.00	0.43	0.53
DLS	0.14	0.06	0.20	0.19	0.27	0.43	0.00	0.04
Zeta potential	0.14	0.07	0.03	0.03	0.08	0.53	0.04	0.00